14p

STELLAR SPECTROPHOTOMETRY FROM ABOVE THE ATMOSPHERE

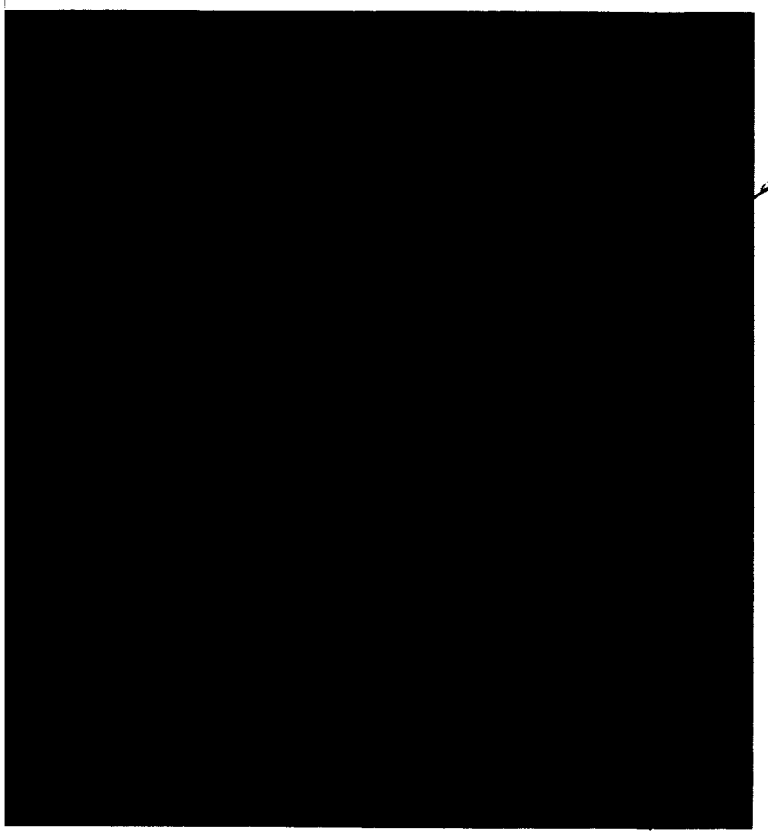

T. P. Stecher and J. E. Milligan

Goddard Space Flight Center
Greenbelt, Maryland

Reprinted with permission from *Astrophysical Journal*, volume 136, number 1, pages 1-13, July 1962

Reprinted from
THE ASTROPHYSICAL JOURNAL
Vol. 136, No. 1, July 1962

STELLAR SPECTROPHOTOMETRY FROM ABOVE THE ATMOSPHERE

THEODORE P. STECHER AND JAMES E. MILLIGAN
Goddard Space Flight Center, National Aeronautics and Space Administration
Greenbelt, Maryland

Received January 24, 1962; revised February 20, 1962

ABSTRACT

Instrumentation was flown in an Aerobee rocket to obtain stellar spectra in the ultraviolet. Stars of spectral type F0 I*a* to O5f and WC7 were observed from λ 1600 to λ 4000. Satisfactory agreement between theoretical model atmospheres and the observations was obtained for the F0 I*a* star throughout the observed spectrum and for the earlier stars down to λ 2600. Below λ 2400 there is a fundamental disagreement between the observations and theory for the hotter stars. It appears that the source of this disagreement is in the atmosphere of the star, and the suggestion is made that it is due to quasi-molecular absorption by various combinations of hydrogen and helium atoms and ions. Attention is drawn to the changes that are necessary in the interstellar radiation field.

I. INTRODUCTION

It has been obvious for some time that the earth's atmosphere prevents a considerable amount of needed astronomical information from being obtained. It has not generally been realized, however, how much information of both qualitative and quantitative nature can be obtained with small, unguided sounding rockets. The coupling of modern electro-optical techniques with sounding rockets sets forth the possibility of obtaining flux measurements on bright stars with an accuracy approaching 1 per cent over a significantly narrow band pass. Rockets with peak altitudes in excess of 150 km spend a considerable portion of their flight time above that region of the atmosphere that contributes to continuous absorption and hence makes possible stellar observations almost anywhere in the spectrum.

The first successful detection of far-ultraviolet radiation from astronomical objects other than the sun was made in 1955 from an Aerobee rocket (Byram, Chubb, Friedman, and Kupperian 1957*a*, *b*). Since that time a number of results from such flights has been reported (Boggess and Dunkelman 1958; Kupperian, Boggess, and Milligan 1958; Byram, Chubb, and Friedman 1961). In each of these flights astronomical observations were made with broad-band photometer systems. While data obtained by such techniques are of great interest to astronomers, they are difficult to analyze theoretically. What is needed are spectroscopic observations of the energy distribution of stars with narrower band passes than are normally employed in filter photometry.

Calculations based on both theoretical predictions and early rocket results showed that observations could be made on the spectra of bright stars with low resolution from

an unguided rocket. For 1 per cent data on the brightest stars with a resolution of 100 angstroms and an integration time of 10 ms, the necessary aperture would be 100 cm^2 if the instrument had an over-all quantum of efficiency of 2 per cent. This paper describes an attempt to measure the absolute spectral-energy distributions of individual stars at wavelengths below 3000 A.

II. THE OPTICAL-MECHANICAL DESIGN

The design objectives of the experiment, along with the engineering performance requirements, were presented to the Institute of Optics at the University of Rochester with the request that several optical-mechanical designs be considered which would meet or exceed the minimum experimental requirements. Several ingenious optical de-

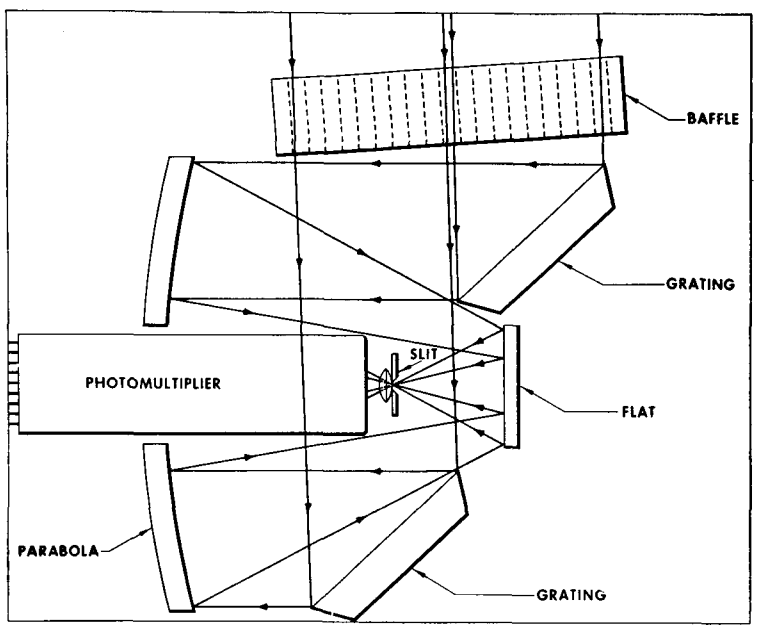

FIG. 1.—Schematic drawing of the spectrophotometers

signs were produced by M. V. R. K. Murty and W. Staudenmaier; the design finally chosen for the experiment was done by the latter (Murty and Staudenmaier 1959). While a complete description of the final optical-mechanical design is being reported elsewhere (Blakney, Murty, Hochgraf, and Staudenmaier 1961), a brief description of it will be given here for completeness.

A schematic drawing of the spectrophotometers used is shown in Figure 1. The optical path is through the baffle to the gratings, where dispersion occurs, on to the parabola, to the flat and on to the slit, where an image of the spectrum of a point source is formed. The spin axis of the rocket is normal to the plane of dispersion of the spectrometer. The spectrum is scanned by the apparent motion of the star due to the rotation of the rocket.

The split mosaic grating feeds the starlight to the parabola so that the detector never vignettes the beam from the parabola. The slit is always on axis in the direction in which dispersion occurs. The parabola is $f/1$ in the plane of dispersion and $f/1.5$ along the slit length, enabling a 3° field of view without serious aberration. The coma at the extremities

of the field is equivalent to 39 A, and the long axis of the coma coincides with that of the slit.

The baffle is a plane-parallel collimator which restricts the field in the direction of dispersion. This was needed to limit the response of the spectrophotometers to first-order dispersion in the spectral range of interest. An extended visible response would give signals on the cooler stars, which would in many cases be superimposed on the ultraviolet signals of interest. The prime need for the baffle, however, was in the attenuation of the zero-order image. The zero-order signal of a star is about fifty times as intense as the signal of a 50 A section of the spectrum of the same star. This being the case, stars more than 6 mag. fainter than the star being observed would contribute 10 per cent signals. Since useful data could be obtained on fourth-magnitude B stars with this system, stars of any spectral class brighter than tenth magnitude would have caused difficulty if their zero-order image were present in the spectrum of a brighter star. On the other hand, the zero-order image of a star provides an excellent wavelength indicator. Given the angular dispersion and the angular velocity of the instrument, the wavelength of any spectral feature can be determined by measurement in time from the zero-order image. The baffle used gave a triangular response centered at λ 2400 and admitted 2 per cent of the zero-order image. It was fabricated from black plexiglass with triangular grooves in the plates, which effectively reduce scattering at small angles.

Two grating solutions were used, in order that the spectral range of interest could be covered with high efficiency and without overlapping spectral orders. A pair of 600 line/mm gratings was used for the spectral range λλ 1225–3000 and a pair of 500 line/mm gratings was used for the region λλ 1700–4000. The 500 line/mm long-wavelength instruments had a dispersion of 267 A per degree. With a slit 3° long and passing 50 A, the instrument would have a monochromatic field of view on the sky of almost one-half square degree.

The gratings were ruled by Richardson at the Bausch and Lomb Optical Company. They had about 65 per cent efficiency at the blazed wavelength in the first order and achieved approximately 80 per cent of theoretical resolving power. The parabolic mirrors were 15 by 23 cm, with a 23-cm focal length. They had a central hole 6 cm in diameter and gave 80 μ images on axis. They were ground at the Naval Weapons Plant. All the optics were coated at the Bausch and Lomb Optical Company. Those for the short-wavelength region received special ultraviolet coatings (Berning, Haas, and Madden 1960), and those for the longer-wavelength region received fast-fired aluminum.

The detectors used for the long-wavelength instruments were E.M.I. 6255S fused-silica windowed photomultipliers. A calcium fluoride field lens was used for forming an image of the entrance aperture on the cathode of the photomultiplier, thus avoiding variations due to cathode sensitivity and electron focusing. The photomultipliers were shielded both magnetically and electrostatically with conetic material. The short-wavelength cutoff was determined by the fused-silica window of the photomultiplier.

The detectors used for the short-wavelength instruments were E.M.I. 9514S glass-windowed photomultipliers upon which a 2-cm-diameter translucent coat of sodium salicylate was deposited in the center of the 5-cm-diameter face plates. Sodium salicylate fluoresces under ultraviolet radiation with a high constant quantum efficiency. The fluorescent light is in the blue and is therefore detected by the glass-windowed photomultiplier. A polished aluminum reflector was placed between the slit and the photomultiplier in such a manner as to return most of the light fluoresced in the backward direction into the photomultiplier. A quantum efficiency for the ultraviolet detector of about 5 per cent from λ 3000 down was achieved in this manner. A cleaved calcium fluoride crystal was placed behind the slit to restrict the response of the instrument to wavelengths longer than λ 1225. This was done to eliminate the response to hydrogen Lyman-α from the solar system, the intensity of which is comparable to that of the strongest star signals expected with this kind of objective system. The dark current of

all the photomultipliers was a factor of a thousand below the full-scale output of the amplifiers.

The decision was made to fly two far-ultraviolet and two near-ultraviolet instruments. The optimum mechanical arrangement for best coverage of the sky was to pair the two types of instruments and to mount the pairs 180° from each other. One pair had 50 A resolution, and the other had 100 A resolution. The mechanical design for mounting the optics was done by N. Hochgraf at the Institute of Optics.

The major problem of the mechanical design was to mount the 30 pounds of glass in a cylindrical section 36 inches long with a weight limitation of 100 pounds total. Structurally, the glass is an inert mass, and this adds to the vibration problems, as well as the steady-state gravitational loading under acceleration.

The final mechanical design mounted the optics for each instrument on identical plates. A stepped two-armed channel then supported the individual instruments. The use of a different-sized mounting block for each step allowed the easy removal of the spectrophotometers for calibration and made it possible to interchange them if necessary. The skin of the rocket passed over the channel, with physical contact occurring only at the base ring and rubber shock mounts at the top. There was a door for each pair of spectrophotometers, which was designed to be opened when the rocket was above the atmosphere. The baffles were spring-mounted to extend through the doors when the doors were opened. The baffles were firmly stopped in the proper position. Almost all the mechanical structure was fabricated from magnesium.

Considerable concern was raised over the possibility of the mosaic grating system becoming misaligned because of vibrational resonances. Extensive vibrational tests were conducted. Resonances up to 200g were measured on the grating mounts in the 50–150 cycle per second range when the whole instrument was vibrated with a 10g sinusoidal input. Although the instruments maintained their alignment under these tests, modifications were made to tie together mechanically the various optical mounts which had different resonant frequencies, so that they provided mutual vibrational damping. Finally, the whole instrument successfully withstood 1 minute of white noise at the 10g level.

III. ELECTRONIC INSTRUMENTATION

The 83-inch ogive nose cone contained the electronics and telemetry and included all the components necessary for the proper function of the rocket and the instrumentation, along with the miscellaneous function data necessary to interpret the various aspects of the experimental result. The total weight was 100 pounds. Straightforward electronic techniques were generally used. These methods have been widely described in the engineering literature and therefore will not be discussed here. Of particular interest, however, are the amplifiers and the high-voltage supplies for the photomultipliers.

The amplifier was a modification of the transistor version of the electrometer designed by Pragland and Nichols (1960). The sensitivity was reduced to 1×10^{-7} amp. full scale, and the frequency response was optimized for this experiment at 83 cycles per second. A ten-gain, low-impedance, temperature-compensated voltage amplifier was added to the basic electrometer so that two independent outputs, which differed by a factor of 10 in sensitivity, were obtained from one photomultiplier input. The stability of these units is comparable to the best laboratory electrometers now available.

The high-voltage power supplies were basically transistor oscillator dc to dc converters with corona regulators in the output filter circuit. These were regulated to better than 0.1 per cent. A separate one was used for each photomultiplier.

IV. THE ROCKET AND ITS ASPECT

The rocket, NASA 4.11, was an Aerobee 150A. This is a four-fin ballistic missile designed to be launched from the Wallops Island, Virginia, tower. It is a liquid-fueled

rocket with a solid booster. The fuel is a 65–35 mixture of aniline and furfural alcohol, and the oxidizer is red fuming nitric acid, which is forced by a high-pressure helium tank into the engine, where it is hypergolic. The rocket is guided for the first 160 feet by rails in the tower, then it is spin-stabilized. The whole tower can be pointed in azimuth and elevation to control the impact point under varying wind and range conditions.

To the basic rocket there was added the 36-inch optical extension, the 83-inch ogive nose cone, and a de-spin system using a rate switch and the leftover helium from the high-pressure tank. The de-spin system slows the rotation after burnout to a preselected rate. This rate was chosen to be compatible with the number of photons expected and with the expected dynamic behavior of the rocket.

The rocket was fired at 0342 E.S.T., November 22, 1960, after a 6-hour countdown. The peak altitude was 107 miles, giving a total of more than 400 seconds of telemetry. It was launched on an azimuth of 110° with an elevation to give an effective 87° in the light, steady wind. The launch time was selected to provide the highest probability of acquiring data in the winter Milky Way. The rocket spin-rate reached a maximum of 3.1 r.p.s. during powered flight. It was then de-spun to 0.054 r.p.s. By the time data acquisition was begun, all aerodynamic forces had ceased, and the rocket followed the laws of a rigid body in a uniform gravitational field. The rotation of the rocket caused a swath the length of the slit to be swept out on the celestial sphere. The spectrum of any star in this swath was obtained as a result of this motion. The precession of the rocket displaced the projected path of the slit on the celestial sphere on the next rotation. In this manner a large portion of the sky was scanned. The only problem was to know where the spectrometer was pointed at any instant of time.

The determination of a rocket's aspect is straightforward but sometimes difficult. On this rocket an orthogonal pair of flux-gate magnetometers was mounted to sense the component of the earth's magnetic field along the longitudinal axis and the lateral axis of the rocket. Knowing the magnetic-field vector at the launch site and applying the inverse-cube law with altitude, the orientation of the magnetometers could be determined to within a few degrees at each instant of time. The lateral magnetometer was aligned with a spectrophotometer pair. A visual photometer was mounted in line with each of the spectrophotometer pairs. Each photometer had a field of view 3° wide and 6° long. There was a wire across the diagonal of the focal plane which allowed a position determination to be made for point sources moving within the field. Finally, the zero order of the spectrometers provided a position marker only $\frac{1}{6}$° wide in the roll direction.

The determination of the aspect involved the spin rate, the precession rate, and the radius of precession around the angular momentum vector. These quantities are a function of the ratio of the moments of inertia of the rocket. This ratio must be either measured or found by successive approximations in trial aspect solutions. In this case the moments of inertia of the complete rocket were measured prior to launch by the bifilar pendulum method. The measured ratio was found to be 145, which also gave the best fit with the star positions in the final aspect solution.

The final aspect solution was made on an LGP-30 digital computer with a program written by A. Boggess III. The computer solution obtained with the observed data predicted the positions of twenty bright stars within half a degree of their true positions. One star, α Leonis, was observed late in the flight, and the solution was several degrees away from its true position. The onset of aerodynamic forces was undoubtedly the cause of this. The identification of α Leonis is certain from intensity and spectral information, as well as the proximity of the aspect solution.

Optimum dynamic behavior was attained by this rocket. Upon the completion of despin the precession circle for the rocket nose was tangent to the launch azimuth. The precession rate was 0°.45/sec, the precession radius was 73°, the spin rate was 18°.64/sec. The angular zenith distance of the longitudinal axis was 13° initially and went to a distance of 134° at the termination of the free-fall portion of the flight.

V. CALIBRATION

Two methods of calibration were used: a calculated one and a completely empirical one. The calculated one was made by using measured reflectivities from test plates made at the same time that the mirrors were coated. The gratings were supplied with three monochromatic efficiencies in the region of interest. The relative spectral response of the photomultipliers was taken as an average value from a previously measured group of tubes. As the dispersion for the group of tubes was small and primarily due to variations in the transmissions of the fused-silica face plate, the error was reasonably small. To this were added the transmission of the baffle and the vignetting of the various structural elements.

The laboratory calibration was done with a 40-cm concave-grating vacuum monochromator to which a 5-foot tube, 6 inches in diameter, was attached. The other end of the tube was attached to a circular tank 18 inches in diameter. The tank contained electrical fittings and a turntable, which could be rotated while under vacuum. The grating of the monochromator was diaphragmed down to produce a $f/100$ beam, and the exit slit was opened to 30 A. A free-flow molecular hydrogen-discharge lamp was used as the light-source. A stable current-regulated power supply was used with the lamp.

The basic calibration procedure was to set the monochromator on a wavelength, rotate the spectrophotometer being calibrated until the maximum signal was found, and then the current output of the photomultiplier was measured. The procedure was then repeated at another wavelength. When a sufficient number of points in the spectrum had been measured, the spectrophotometer was replaced with a glass-windowed photomultiplier which had been coated with sodium salicylate, and the same wavelengths were measured again. Sodium salicylate fluoresces in the blue when ultraviolet light falls upon it. It has been measured to have a constant quantum efficiency (Johnson, Watanabe, and Tousey 1951) from λ 584 to λ 3200. The ratio of the outputs of the sodium salicylate photomultiplier and the instrument under test gives the relative spectral response of that instrument. To place the relative sensitivity of the spectrophotometers on an absolute basis in terms of ergs $cm^{-2}\,sec^{-1}\,A^{-1}$, it is only necessary to measure its absolute response at one wavelength and multiply by the ratio of the photon energies at that one wavelength and the wavelength being considered. This final monochromatic calibration was performed with a calibrated point-source mercury lamp filtered to give only λ 2537. This final calibration was made at a large distance, so that effectively parallel light filled the optics, which at that time were mounted in flight condition.

The primary difficulty with the method as outlined was that it was impossible to fill the optics of the spectrophotometers with a sufficiently parallel beam from the monochromator. Since the response of all the components was high and a smooth, slowly varying function of wavelength, this difficulty is unlikely to have seriously modified the response-curve. The calculated curve and the measured response agreed within 10 per cent at all wavelengths.

The response of the instruments was measured from λ 3000 to the short-wavelength cutoff. The response to wavelengths longer than λ 3000 was taken from the calculated curves and combined with a forced fit of observed stars with several model atmospheres. The calibration in the region λλ 1800–2800 is probably within 10 per cent, while the calibration outside this range is likely to be somewhat poorer. Each spectrometer prior to calibration and until the actual firing was kept in a continuously flowing atmosphere of dry nitrogen.

VI. THE DATA

Detailed examination of the instrumentation performance monitoring channels on the telemetry records showed that all the instrumentation was operating in proper fashion. Signals from about 30 stars were recorded on the two long-wavelength spectrometers, but the two short-wavelength instruments were saturated throughout flight. Of the sig-

nals recorded, those for seven stars were of good quality throughout the spectral range of interest, and another eight contained some useful information. The remaining signals were either the zero-order signals from cool stars or ones that were lost in the background, which always amounted to more than a 15 per cent deflection with a strong north-south asymmetry.

The sensitivity of an objective dispersive system to high surface brightness is such that the presence of a visual aurora would have canceled the flight. At the time of the flight no obvious aurora could be seen by the naked eye from the launch site. However, postflight information on the state of the ionosphere, coupled with the data both from the visual photometers and from the ultraviolet spectrometers aboard the rocket, indicated that the rocket flew into a very strong ultraviolet aurora which had a very faint visual counterpart. The aurora was a geometrically quiescent phenomenon, and thus its only effect on the stellar spectra was to give a reduced signal-to-noise ratio. This aurora was apparently related to the complex series of solar events which occurred during the month of November. A detailed description of the phenomena observed will be the subject of a note to be published elsewhere.

A tabulation of the stars for which some useful data were obtained follows, along with their visual magnitudes and spectral types, from a catalogue by Miss Woods (1955), who has classified all the observed stars. An estimate of the quality versus wavelength is given, along with any special reduction problems. Each instrument observed a given star once. The following stars were observed with 50 angstrom resolution.

α Carinae, F0 Ia, V = −0.72 good signal.—The zero order was in the saturated southern airglow. The wavelength scale was determined from the H and K lines and the long-wavelength cutoff. A correction was made starting at λ 2600 for the curvature in the airglow background near the southern horizon. This was accomplished by utilizing data from the preceding and following scans across the southern horizon.

γ Orionis, B2 IV, V = 1.64 good signal.—There is an overlap with δ Orionis shortward of λ 2700. A correction was made on the basis of Traving model atmosphere (T_e = 37950, log g = 4.45) and visual magnitude for the region around λ 4000 on δ Orionis.

δ Orionis, O9.5 III, V = 2.2 good signal.—There was overlap all the way through with γ Orionis and ι Orionis. This star gives an upper limit to the flux in the λ 2000 region only.

ι Orionis, O9 V, V = 2.74 good signal.—The spectrum is blended longward of λ 3000 with δ Orionis but relatively good on the short side. The zero order is not clear.

β Canis Majoris, V1 II, V = 1.97 excellent signal.—The best observation made.

α Canis Majoris, A1 V, V = −1.44 mostly saturated.—It becomes saturated at λ 4000 and returns at λ 1800. The zero-order signal is also saturated.

ε Canis Majoris B1 II, V = 1.43 excellent signal.—The zero-order signal from α Canis Majoris appears at λ 3300.

τ Canis Majoris O9 V = 4.36 fairly poor signal.—The spectrum overlaps at the short wavelengths with η Canis Majoris with a separation of 1200 A.

η Canis Majoris B5 Ia, V = 2.40 poor signal.—This spectrum was only usable short of λ 2800.

γ Velorum WC7, *V = 1.98 excellent signal.*—There is a considerable variability in the stellar background in this part of the sky. The zero order was close to the horizon. The r.m.s. noise in signal level was considerably higher than it would have been for a smooth source, indicating that emission lines were present.

α Leonis B8 V, V = 1.36 good signal.—The long-wavelength (λ > 3600) end overlapped with η Leonis, and no correction was made.

The following were obtained with the 100 A instrument, which had a considerably poorer signal-to-noise ratio:

β Orionis B8 Ia, V = 0.21 fair signal.—The spectrum was saturated down to λ 2200.

α Carinae FO Ia, V = −0.72 fair signal.—This was saturated in the long-wavelength

region. The agreement between the 100 and the 50 A scans on this star was very good below 3000 A.

o^2 *Canis Majoris B3 Ia, V = 3.00 poor signal.*

λ *Orionis O8, V = 3.49 poor signal.*

ζ *Puppis O5f V = 2.2.*—This overlapped with γ Velorum and was saturated over a good part. The flux around λ 2000 could be assigned an upper limit.

Figures 2 and 3 are a reproduction of the FM-FM telemetry traces for the seven stars for which good data were obtained. Once the stars have been identified through the aspect solution, the reduction of the data is straightforward and quite similar to tracings obtained in other astronomical investigations. The DKT-7 PPM and FM-FM transmitters both had an in-flight calibration system and can easily be read to accuracies exceeding 1 per cent. In the case of the 50 A quartz instrument, a channel was available from each transmitter, and the data were read from each.

In general, the wavelength scale was determined from the zero-order signal and the scanning rate of the spectrometer. The scanning rate was 5000 A/sec. The data were read with an automatic data-reducing instrument at 25 A intervals and then plotted. A smooth curve was then drawn through the points, and the data were tabulated at 100 A intervals. This value was then multiplied by the calibration factor for the corresponding wavelengths, in order to obtain the stellar fluxes in terms of ergs cm^{-2} sec^{-1} A^{-1}. The mean error due to the statistical nature of the detected photons is 2.8 per cent per hundred angstroms for a stellar deflection of 60 per cent of full scale on the telemetry when this deflection is superimposed on a 20 per cent background. The assessment of errors with respect to the absolute calibration is considerably more difficult and is dependent on both the absolute calibration and the error in positioning of the continuous background but should not exceed 30 per cent for the stars in Table 1. Spectral features are

TABLE 1

STELLAR FLUX IN ERGS CM^{-2} SEC^{-1} A^{-1} $\times 10^{+9}$

λ	Cal. $\times 10^9$	ϵ Canis Majoris	β Canis Majoris	γ Velorum	α Leonis	α Carinae	γ Orionis	ι Orionis
1600	111	2.2	.....	21	.....	.....	.....	11
1700	21.3	1.7	2.3	7.6	0.9	.....	2.8	11
1800	9.51	1.2	2.9	6.2	1.1	.....	3.6	9.3
1900	6.08	1.0	3.2	5.2	1.3	.....	3.8	8.5
2000	4.67	1.3	3.5	7.5	1.5	0.5	3.7	7.7
2100	4.15	2.9	3.9	7.4	2.0	1.0	4.5	8.5
2200	3.86	6.5	4.6	8.1	2.5	0.8	6.1	8.9
2300	3.69	8.6	5.5	9.0	2.9	1.9	6.5	9.5
2400	3.54	9.3	5.6	11.7	3.1	1.4	4.8	8.9
2500	3.57	8.5	5.3	9.1	3.1	1.4	5.5	6.6
2600	3.74	8.1	4.9	8.5	3.0	2.1	5.2	8.4
2700	3.78	7.2	4.3	7.8	2.8	1.5	4.8	7.6
2800	3.83	6.5	3.6	7.1	2.6	2.1	4.2	7.0
2900	3.74	5.8	2.8	6.4	2.4	2.3	3.6	6.2
3000	3.74	5.3	2.5	5.8	2.2	3.0	3.2	5.8
3100	3.80	.....	2.4	5.2	2.2	3.2	3.0	.....
3200	3.89	.....	2.2	4.4	2.1	2.3	2.6	.....
3300	4.04	.....	2.0	4.3	2.1	2.7	2.3	.....
3400	4.38	.....	1.8	4.2	2.1	2.9	2.2	.....
3500	4.52	.....	1.7	3.9	2.1	2.8	1.9	.....
3600	4.93	3.2	1.6	3.7	.....	3.8	1.8	.....
3700	5.33	3.4	1.4	3.6	.....	5.1	1.6	.....
3800	6.11	3.3	1.4	3.8	.....	11.5	1.8	.....
3900	7.35	3.1	1.4	3.8	.....	13.3	2.1	.....
4000	8.88	2.9	1.2	3.8	.....	18.1	1.4	.....
4100	11.5	2.6	0.9	3.9	.....	14.4	0.5	.....

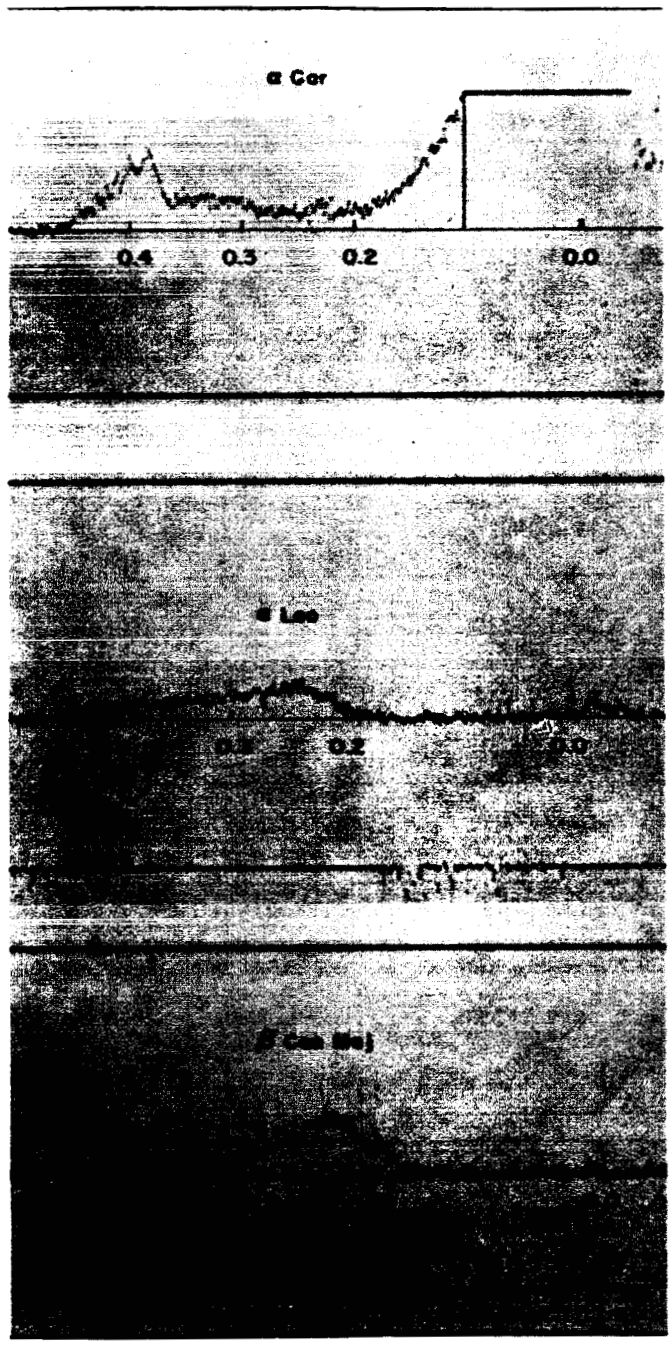

FIG. 2.—FM–FM telemetry traces for α Carinae, α Leonis, and β Canis Majoris. The wavelength is given in microns. The resolution is 50 A, and the scanning rate is 5000 A/sec. The saturated signal to the right of α Carinae is the southern airglow horizon.

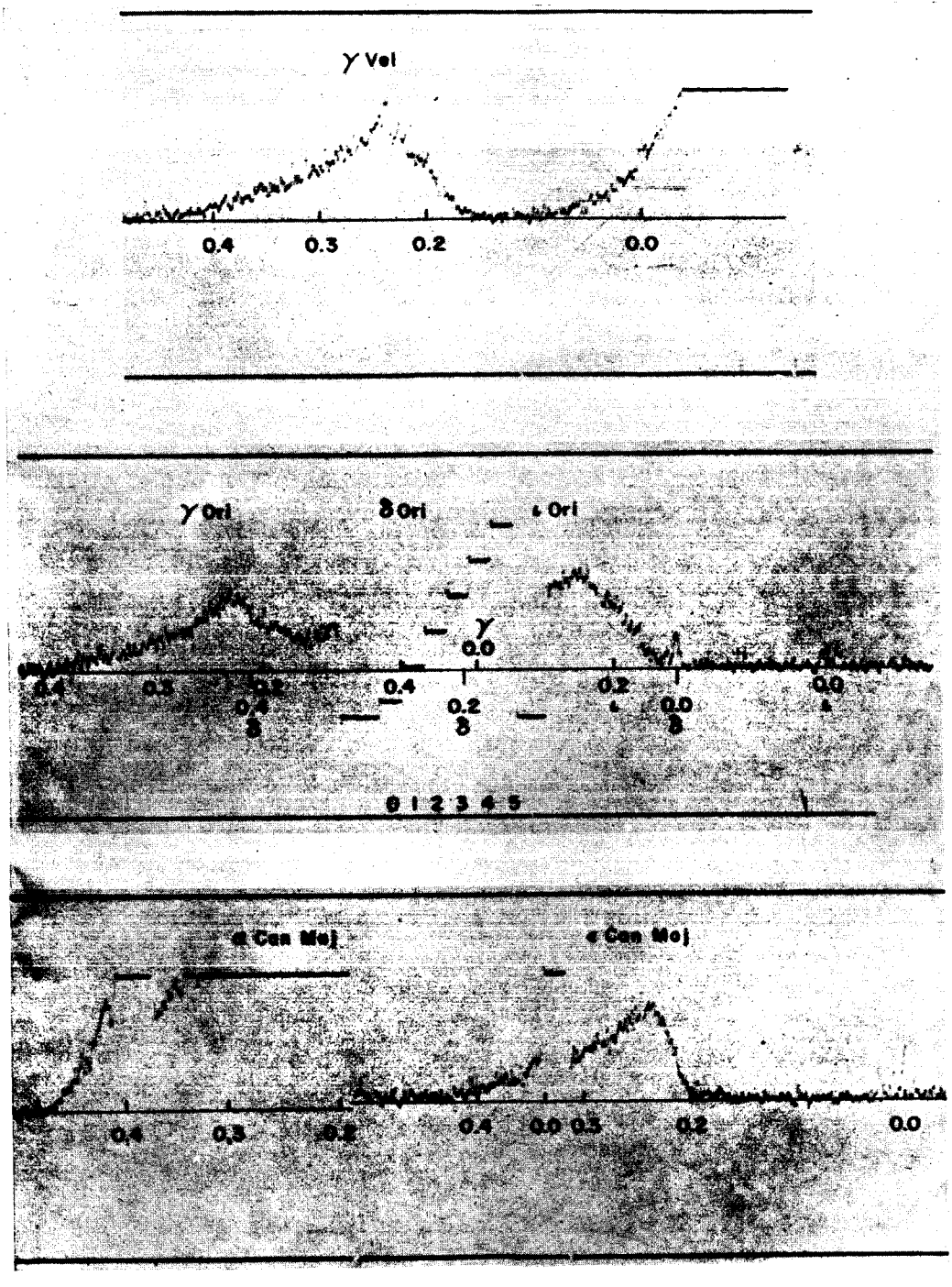

FIG. 3.—FM-FM telemetry traces for the indicated stars. The resolution is 50 A and the scanning rate is 5000 A/sec. The telemetry calibration of 0–5 volts appears in the spectrum of δ Ori.

hard to discern in the traces because of the low resolution and noise from the background. Noise pulses due to cosmic rays in the photomultiplier and to stimulated emission in the atmosphere have a width only half as wide as any feature in the spectrum of a star. Inspection of Figures 2 and 3 will indicate the possible presence of emission and absorption lines.

The absolute stellar fluxes for the stars appearing in Figures 2 and 3 are presented in tabular form in Table 1. The first column in Table 1 is the wavelength. The second column contains the factor by which the deflection due to the stellar signal in terms of volts on the telemetry has been multiplied to obtain the stellar fluxes in terms of ergs cm^{-2} sec^{-1} A^{-1} for the corresponding wavelength. The remaining columns contain the individual star data in ergs cm^{-2} sec^{-1} A^{-1}.

VII. DISCUSSION

For the purpose of discussion, selected observations are presented in graphical form and compared with representative model atmospheres. The model atmosphere has been arbitrarily normalized at λ 2600 in each case. Figure 4 shows the observed spectrum of

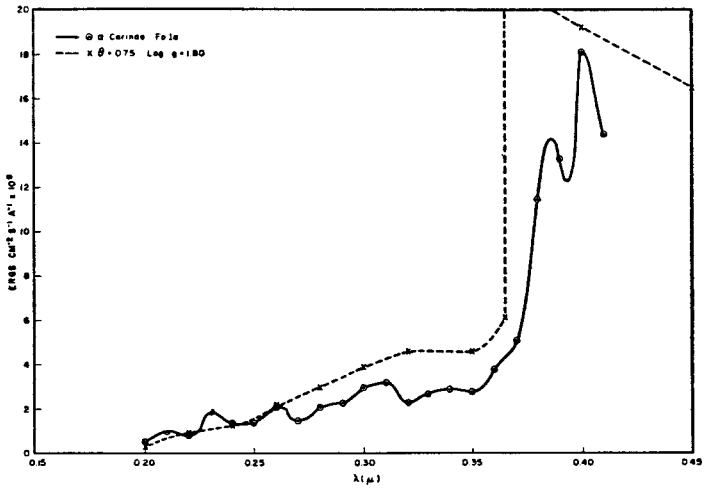

FIG. 4.—The solid line is the observed absolute flux of α Carinae, F0 Iα. The dashed line is a model atmosphere for $\theta = 0.75$ and log $g = 1.80$. The theoretical flux-curve (Canavaggia and Pecker 1953) has been arbitrarily normalized to the observed one at λ 2600.

α Carinae F0 Iα with a model atmosphere computed by Canavaggia and Pecker (1953) which is assumed to represent F0 supergiant. The fit is reasonably good over the range of interest when it is realized that line blanketing is not included in the model.

In Figure 5 we compare ε Canis Majoris B1 II with Miss Underhill's Model III (Underhill 1957), which is for $T_e = 28470$ and log $g = 3.80$. Inspection shows that the slope of the flux as a function of wavelength of the model is in fundamental disagreement with the observation below λ 2400. The monochromatic difference at λ 1800 is a factor of 30.

In Figure 6 α Leonis B8 V is compared with Saito's (Saito 1956) model for $T_e = 15500$ and log $g = 3.80$. Again the slopes below λ 2400 are in disagreement. At the long-wavelength end (λ > 3600) the discrepancy is caused by a blend with η Leonis which has not been corrected.

Figure 7 compares the absolute flux of ε Canis Majoris and β Canis Majoris. While both are in disagreement with models intended to represent early stars, they are also

different from each other by a factor of 5 at λ 2000 when normalized at longer wavelengths.

Every star observed, with the sole exception of α Carinae, is deficient in flux below λ 2400 from that predicted by model atmospheres by a factor which considerably exceeds the photometric errors or the choice of models. The deficiency in flux may be considered to be either an intrinsic property of the star or due to an absorber in the interstellar media. Let us first consider the latter as a hypothesis.

The stars observed have little or no color excess and are, for the most part, close to the sun and do not appear on lists for interstellar lines. α Canis Majoris is down a factor

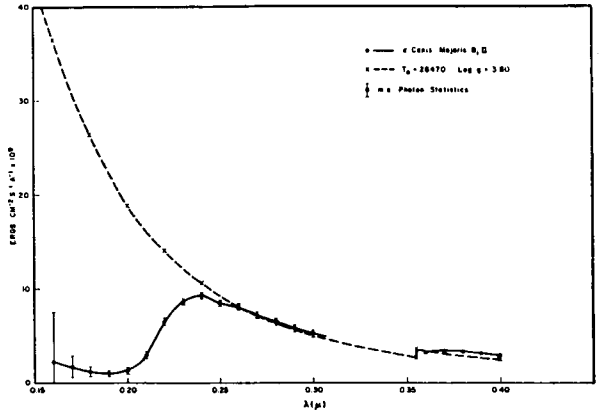

FIG. 5.—The solid line is the observed absolute flux of ε Canis Majoris, B1 II. The dashed line is a model atmosphere for $T_e = 28470$ and log $g = 3.80$. The theoretical flux curve (Underhill 1957) has been arbitrarily normalized to the observed one at λ 2600. The mean-error flags are for the photon statistics averaged over 100 A intervals.

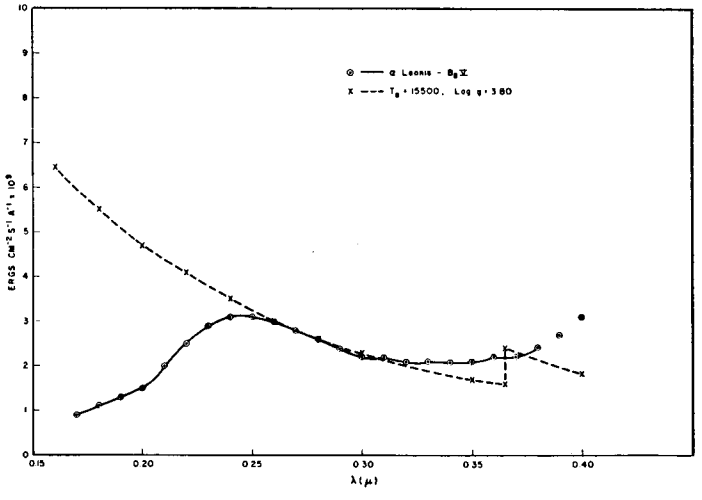

FIG. 6.—The solid line is the observed absolute flux of α Leonis, B8 V. The dashed line is a model atmosphere for $T_e = 15500$ and log $g = 3.89$ (Saito 1956) and has been arbitrarily normalized to the observed flux-curve at λ 2600. The long-wavelength end is blended with η Leonis.

of 10 at λ 1800 with respect to Osawa's A3 V model (Osawa 1956), while α Carinae at eight times the distance does not show the effect.

If the model is assumed to be correct and the absorption is assumed due to a circumstellar cloud, the problem becomes one of absorbing more than half the total flux of the star without some evidence of this cloud appearing in the visible. The only absorbing mechanisms that would have greater efficiency at low densities than in the stellar atmospheres are those involving the metastable levels of atoms or the formation of solid particles. The only abundant atom with a metastable level in the region of interest is helium 2^3S. This would start absorbing at λ 2600, following approximately a ν^{-1} law (Huang 1948) instead of the positive exponent starting at λ 2400 which the observations suggest.

The number of molecules necessary to produce the observed absorption would have to exceed 10^{-2} cm^{-3} through the path to the star. As the hydrogen molecule does not absorb

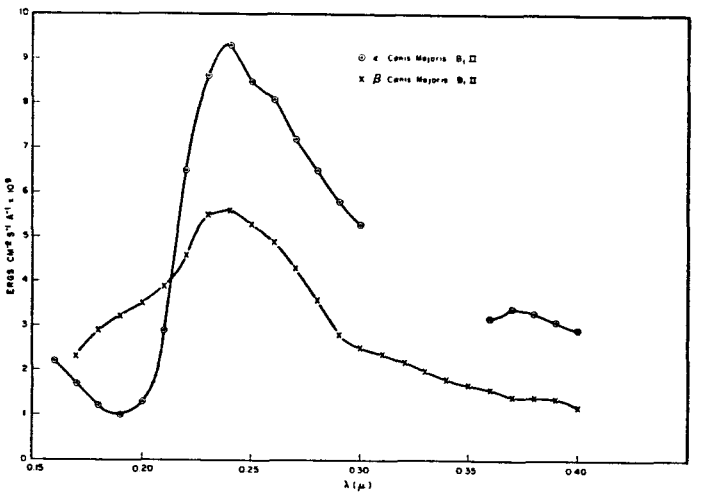

FIG. 7.—The circles are the observed absolute flux of ε Canis Majoris, B1 II. The crosses are the absolute flux of β Canis Majoris, B1 II.

in this region of the spectrum and other common molecules have a density on the order of 10^{-8} cm^{-3} (Bates and Spitzer 1951), this explanation may be ruled out. Bound-free absorptions from atomic species in the interstellar medium can be ruled out by abundance considerations. Interstellar grains are also unlikely, since this would require them to all be of the same size on the basis of the sudden start at λ 2400. In addition, their abundance is too small. It appears that the observed lack of flux cannot be due to interstellar absorption, and therefore we must consider the atmosphere of the star itself.

Since the flux is less than that predicted for each star from A1 V to O5f by about an order of magnitude, it seems unlikely that a single source of opacity could be the cause in each case.

In Figure 5 the increase in flux in the model at shorter wavelengths is due to the form of the absorption coefficient of neutral hydrogen, which varies as ν^{-3}, and to the scattering by free electrons, which is independent of frequency. The form of the observed flux-curve below λ 2400 is suggestive of a molecular absorption or the sudden commencement of line blanketing. The continuous atomic processes that contribute to the opacity in a stellar atmosphere are generally well understood and have been taken into consideration

in the computation of stellar atmospheres (Vitense 1953) and therefore do not present an explanation.

Picket-fence line blanketing by metallic lines would hardly be expected to start suddenly at λ 2400, as inspection of ultraviolet multiplet tables show about as many lines just above this wavelength as below. Gaustad and Spitzer (1961) have computed ultraviolet line absorption for a B2 star and find it unimportant with respect to the effect found here.

Greenstein (1948) has suggested from simple considerations that Lyman-α in the sun would have an equivalent width of 10000 A. However, the number of neutral hydrogen atoms would appear far too small in the hotter stars for this to be of importance, even on the basis of simple theory.

Goldberg and Pierce (1959) have suggested that picket-fence blanketing by NO and CO may be the cause of the opacity in the sun below λ 1800. Their high dissociation energy would allow a high concentration in the late A stars, but at higher temperatures they would all be dissociated and the constituent atoms ionized.

One possible source of opacity that has been generally neglected is that due to quasi-molecules. Electronic transitions during the process of collision between two atoms have a high probability in some cases. For instance, Erkovich (1960) has shown that under certain conditions absorption of the quasi-molecule of H^2 is 10^8 times that of H^- at λ 2000. There are a number of quasi-molecules and molecules that can be found from various combinations of hydrogen and helium atoms and ions. A tabulation of those combinations which have known interaction energies has been made by Fallon, Mason, and Vanderslice (1960).

For stars in which H_2^+ is a known source of opacity H_3^+ should also be considered. H_3^+ has a binding energy of 4.18 ev and a high formation rate (Varney 1960). At somewhat higher temperatures the HeH^+ molecule might be an important source of opacity. It has a stable ground state of 2.2 ev (Coulson and Duncanson 1938), but its optical transitions are unknown.

For HeH^{++} the exact wave functions have been computed for a number of states by Bates and Carson (1956), and some of its properties have been computed by their associates. The 2p σ state is of particular interest, in that it is a partially attractive one. Transitions from it to the 3d σ state have oscillator strengths up to 0.3 that fall in the right regions of the spectrum to cause the absorption observed (Arthurs, Bond, and Hyslop 1957). The rate coefficient for formation directly into the 2p σ state is very high and almost independent of temperature (Arthurs and Hyslop 1957). This process requires the coexistence of doubly ionized helium and neutral hydrogen, which is unlikely to exist in sufficient numbers under the condition of thermodynamic equilibrium in the atmosphere of a star. There are, however, other ways by which the state may be populated.

This particular mechanism, if actually the cause of the absorption, would have interesting consequences on ionization of the interstellar media. The molecule absorbs well below the Lyman limit but re-radiates at λ 304. Since existing model atmospheres have just enough flux in the Lyman continuum to produce the observed ionization of the H II regions, an additional source of opacity would present difficulties unless discrete line radiation is invoked.

The population of higher states in these molecules would be small but might result in faint absorption bands which could be observed in the visible. The λ 4430 band and other similar bands (Butler and Seddon 1958) can probably also be interpreted as originating in the star as well as the interstellar media. If they are in the star, this would constitute a test for any molecule for which good wave functions are available for higher states.

The large departure of the observed flux from that predicted by model-atmosphere calculations will considerably change the interstellar radiation field in H I regions. For example, since sodium is ionized primarily by the flux occurring in the λλ 1800–2400 region, the discrepancy between the predicted and observed interstellar Ca/Na abun-

dance ratio (Seaton 1951) will be considerably lessened. The actual recalculation of this radiation field will be the subject of another paper.

The authors wish to thank J. E. Kupperian, Jr., E. Serra, W. Gallo, H. Richard, W. Freeman, W. Russell, R. Fiorelli, G. Baker, and A. Stober, of the Goddard Space Flight Center, and N. Hochgraf, R. Horner, W. Staudenmaier, M. V. R. K. Murty, R. Blakney, and K. Teagarten, of the University of Rochester, for their contributions to the project.

REFERENCES

Arthurs, A. M., Bond, R. A. B., and Hyslop, J. 1957, *Proc. Phys. Soc. A*, **70**, 617.
Arthurs, A. M., and Hyslop, J. 1957, *Proc. Phys. Soc. A*, **70**, 849.
Bates, D. R., and Carson, T. R. 1956, *Proc. R. Soc. London, A*, **234**, 207.
Bates, D. R., and Spitzer, L., Jr. 1951, *Ap. J.*, **113**, 441.
Berning, P. H., Haas, G., and Madden, R. P. 1960, *J. Opt. Soc. America*, **50**, 586.
Blakney, R. M., Murty, M. V. R. K., Hochgraf, N., and Staudenmaier, W. 1961 (in press).
Boggess, A., and Dunkelman, L. 1958, *A.J.*, **63**, 303.
Butler, H. E., and Seddon, H. 1958, *Pub. R. Obs. Edinburgh*, Vol. 2, No. 4.
Byram, E. T., Chubb, T. A., and Friedman, H. 1961, *Mém. Soc. R. Sci. Liège*, 5th ser., **4**, 469.
Byram, E. T., Chubb, T. A., Friedman, H., and Kupperian, J. E., Jr. 1957*a*, *The Threshold of Space*, ed. M. Zelikoff (London: Pergamon Press), p. 203.
———. 1957*b*, *A.J.*, **62**, 9.
Canavaggia, R., and Pecker, J. C. 1953, *Ann. d'ap.*, **16**, 47.
Coulson, C. A., and Duncanson, W. E. 1938, *Proc. R. Soc. London, A*, **165**, 90.
Erkovich, S. P. 1960, *Opetka i Spektr.*, **8**, 307.
Fallon, R. J., Mason, E. A., and Vanderslice, J. T. 1960, *Ap. J.*, **131**, 12.
Gaustad, J. E., and Spitzer, L., Jr. 1961, *Ap. J.*, **134**, 771.
Goldberg, L., and Pierce, A. K. 1959, *Hdb. d. Phys.*, ed. S. Flügge (Berlin: Springer-Verlag), **52**, 38.
Greenstein, J. L. 1952, *The Atmospheres of the Earth and Planets*, ed. G. P. Kuiper (2d ed.; Chicago: University of Chicago Press), chap. iv, p. 112.
Huang, S. S. 1948, *Ap. J.*, **108**, 354.
Johnson, F. S., Watanabe, H., and Tousey, R. 1951, *J. Opt. Soc. America*, **41**, 702.
Kupperian, J. E., Jr., Boggess, A., and Milligan, J. E. 1958, *Ap. J.*, **128**, 453.
Osawa, K. 1956, *Ap. J.*, **123**, 513.
Praglin, J., and Nichols, W. A. 1960, *Proc. I.R.E.*, **48**, 771.
Saito, S. 1956, *Contr. Inst. Ap. U. Kyoto*, No. 69.
Seaton, M. J. 1951, *M.N.*, **111**, 368.
Staudenmaier, W., and Murty, M. V. R. K. 1960, *Institute of Optics Semi-annual Research Rept.*, Vol. 1 (Rochester, N.Y.: University of Rochester).
Traving, G. 1957, *Zs. f. Ap.*, **41**, 215.
Underhill, A. B. 1957, *Pub. Dom. Ap. Obs. Victoria*, **10**, 357.
Varney, R. N. 1960, *Phys. Rev. Letters*, **5**, 559.
Vitense, E. 1951, *Zs. f. Ap.*, **28**, 81.
Woods, M. L. 1955, *Mem. Comm. Obs. Canberra*, No. 12.

NASA-Langley, 1963